ELSEVIER

Journal of Molecular Catalysis A: Chemical 184 (2002) 19–29

JOURNAL OF MOLECULAR CATALYSIS A: CHEMICAL

www.elsevier.com/locate/molcata

Supported rhodium thiolate complexes as catalyst precursors for the hydroformylation of 1-heptene in organic media

S. Rojas*, P. Terreros, J.L.G. Fierro

Instituto de Catálisis y Petroleoquímica, CSIC, Cantoblanco, 28049 Madrid, Spain

Received 15 August 2001; accepted 27 November 2001

Abstract

The rhodium thiopyrimidine complex $[Rh(SPymMe_2)(CO)_2]$ was tethered to chemically modified SiO_2 substrates and tested as a catalyst in the hydroformylation reaction of 1-heptene. Catalytic performance was monitored under different reaction conditions for several cycles, and compared with the catalytic behaviour of the Rh thiolate complex in a homogeneous medium. Anchoring of the rhodium complex to the modified SiO_2 surface was performed by displacement of a CO ligand of the rhodium complex by a PR_3 group, following a reaction pathway previously described for gem–dicarbonilic complexes. The XPS data revealed that the sulphur atom is released from the external surface of the solid catalyst during the hydroformylation reaction. However, the thiolate complex is still present in the inner pore network of the solid after the hydroformylation reaction.

Keywords: Rhodium thiolate; Hydroformylation; Supported catalyst

1. Introduction

The accessibility of readily recyclable catalysts is mandatory if suitable industrial catalysts are to be obtained. Within industrial homogeneous catalytic reactions, the hydroformylation of olefins is a major process [1]. The reaction is typically catalysed by organometallic (or coordination) complexes and conducted under homogeneous conditions, which involves a costly catalyst recycling procedure, and consequently the process is expensive. In order to overcome this problem, several alternatives have been developed. The main approach is the heterogenisation of the catalytic process by the use of two immiscible liquid phases [2,3]; typically, one of them is water [4,5]. The hydroformylation of low-chain alkenes (usually C3) in a biphasic medium, performed with rhodium catalysts modified with sulphonated ligands, is the only alternative that has found industrial applications [6]. However, in the field of the hydroformylation of higher alkenes ($C > 6$), this approach involves important technical pitfalls, which mainly arise from the sparing solubility of these higher alkenes in the aqueous phase, in which the catalyst is present [7,8]. In order to avoid catalyst loss, other alternatives are still under study. Currently, there is a large body of work on the anchoring of homogeneous catalysts on solid supports such as SiO_2 or Al_2O_3 [9] organic polymers [10], zeolites [11], activated carbons [12] and, recently, on ZrO_2-modified supports [13,14]. However, several disadvantages are inherent to this type of catalysts, such as the low *n*/*i* (normal/branched) ratio of the products (aldehydes) obtained, the complicated synthesis of the catalysts and, mainly, the leaching of

* Corresponding author. Tel.: +34-915854776; fax: +34-915854760.
E-mail address: srojas@icp.csic.es (S. Rojas).

1381-1169/02/$ – see front matter
PII: S1381-1169(01)00524-6

the metal anchored complex while the reaction takes place, thus limiting their application to only a few reaction cycles.

Several rhodium thiolate catalysts have been anchored to phosphine-modified SiO_2 [15–18] and tested in the hydroformylation of alkenes under mild conditions. Under such conditions, these catalysts display good hydroformylation activities with only a moderate loss of Rh during the process. Here we report the synthesis, characterisation and catalytic performance of a rhodium thiolate complex tethered to a previously phosphine-modified SiO_2 support. Some insight into the nature of the anchored species is offered. Attention is also paid to used catalysts with a view of highlighting the factors that control the chemical stability of the active component.

2. Experimental

All manipulations were carried out under a dry oxygen-free nitrogen atmosphere using standard Schlenk techniques. The atomic content on the silica-supported catalysts was measured by inductively coupled plasma (ICP) atomic emission spectroscopy using a Perkin-Elmer 3300 DV device.

2.1. Precursors

$[Rh(SPymMe_2)(CO)_2]$ (where $SPymMe_2$ is the thionate form of the 4,6-dimethyl-2-mercaptopyrimidine) was prepared according to the published methods [19]. Silica Grace 951 ($S_{BET} = 627\,m^2\,g^{-1}$) was purchased from Grace Davison, US. 3-Triethoxysilylethyldiphenylphosphine was prepared by a procedure described previously [20]. The phosphinated silica was prepared from silica (5 g) previously degassed at 473 K and 3-triethoxysilylethyldiphenylphosphine (2 ml) in toluene under reflux for 24 h, filtered off, washed with toluene, and dried under vacuum [21]. Toluene was dried by distillation over Na under N_2 prior to use. All other reagents were commercial samples and were used as purchased.

2.2. Preparation of catalysts

A solution of the rhodium thiolate complex $[Rh(SPymMe_2)(CO)_2]$ (0.127 g) in toluene (20 ml) was added to the phosphinated SiO_2 (0.5 g), previously degassed under vacuum at 323 K for 12 h. The mixture was refluxed for 24 h, after which it was cooled to room temperature and filtered off. The sample was washed with toluene at 323 K until the solutions were colourless. The resulting solid (Rh–P–Si) was dried under vacuum for 1 day at room temperature and kept under nitrogen. The rhodium content measured by ICP atomic emission spectroscopy was ca. 4.5%. Scheme 1 displays the reaction pathway for the reaction of the Rh complex with the phosphinated SiO_2, however other Rh species were also detected in the solid surface as shown in Section 4.

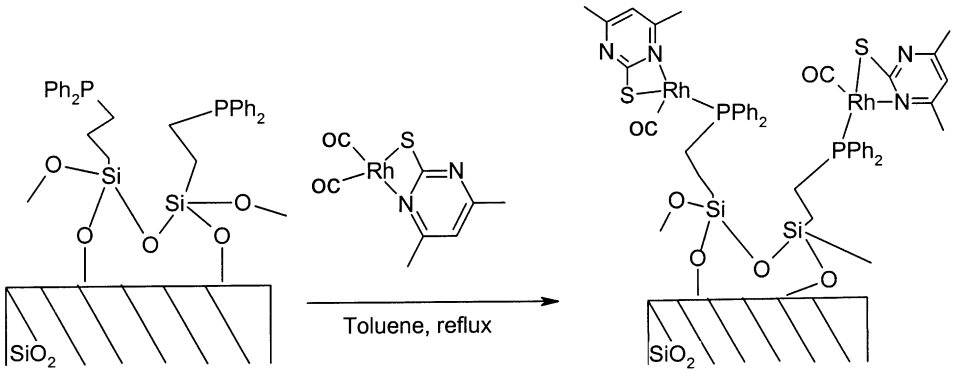

Scheme 1. Tethering pathway of the Rh complex to the modified support by substitution of one CO ligand for a PR_3 fragment (solid Rh–P–Si).

2.3. Characterisation

2.3.1. Determination of specific surface area

N_2 adsorption–desorption isotherms of supports and catalysts were recorded at the temperature of liquid N_2 with a Micromeritics ASAP 2000 apparatus. Samples were previously degassed at 333 K for 24 h. Specific areas were calculated by applying the BET method to the portions of the isotherms within the $0.05 < P/P_0 < 0.30$ relative pressure range.

2.3.2. X-ray photoelectron spectroscopy (XPS)

Photoelectron spectra were acquired with a VG Escalab 200R spectrometer fitted with a Mg Kα ($h\nu = 1253.6$ eV, 1 eV $= 1.6302 \times 10^{-19}$ J) 120 W X-ray source and a hemispherical electron analyser. A DEC PDP 11/53 computer was used for collecting and processing the spectra. The powdered samples were pressed into small stainless steel cylinders and then mounted on a sample rod, placed in a pretreatment chamber, and degassed at 298 K and 10^{-5} mbar for 5 h prior to being transferred to the analysis chamber. Residual pressure during data acquisition was maintained below 3×10^{-9} mbar. The 20 eV energy regions of the photoelectrons of interest were scanned a number of times in order to obtain acceptable signal-to-noise ratio. Intensities were estimated by calculating the integral of each peak, after smoothing, subtraction of the S-shaped background, and fitting the experimental curve to a combination of Lorentzian and Gaussian lines of variable proportions. Accurate binding energies (±0.2 eV) were determined by referring to the C 1s peak at 284.9 eV.

2.3.3. Infrared spectroscopy

Catalytic precursors were characterised by FT-IR spectroscopy over the 4000–400 cm^{-1} region as self-supported pellets. The wafers were prepared by pressing about 10 mg of sample between two mica disks for 5 min under a pressure of 5×10^3 kg cm^{-2}. The equipment used was a Nicolet ZDX Fourier transform-IR spectrophotometer working at a resolution of 4 cm^{-1}. An all-glass cell equipped with greaseless stopcocks and KBr windows were used for the thermal and gas treatments prior to recording the FT-IR spectra.

2.4. Catalytic activity

Catalytic activity measurements were carried out in a 100 ml stainless steel autoclave (Magnedrive Autoclave Engineers). The amount of catalyst was fixed in order to achieve a final Rh concentration of 2×10^{-3} M (equal to that previously used under homogeneous conditions [19]) and was introduced into the reactor and, after pumping out, 1-heptene (1.25 ml) in toluene (25 ml) was added by suction. Carbon monoxide was then introduced (5 or 3 bar, depending on the final pressure value) and the mixture was warmed up to the final reaction temperature. Subsequently, the CO pressure was raised up to 15 or 4 bar and H_2 was added up to 30 or 8 bar, respectively. During the experiment, an equimolar mixture of CO:H_2 was fed to the reactor, keeping the total pressure constant. The reaction mixture was stirred magnetically at 750 rpm. Samples were periodically removed, cooled to 243 K and analysed by gas–liquid chromatography in a Hewlett-Packard HP 6890 chromatograph equipped with an FID detector and a 30 m × 0.32 mm HP-Innowax column. After each experiment, the reaction mixture was filtered out using a cannula system under nitrogen and the solid catalyst was washed with toluene. The reactor was then closed—maintaining a nitrogen atmosphere—dried under vacuum, and used for hydroformylation in a new reaction cycle using the same procedure.

3. Results

3.1. Specific areas and porosity

The BET area of the SiO_2 substrate was 627 $m^2\,g^{-1}$ and decreased to 488 $m^2\,g^{-1}$ upon phosphination. A further decrease in BET to 338 $m^2\,g^{-1}$ was observed upon anchoring the Rh complex. The adsorption–desorption isotherms exhibited hysteresis loops above relative pressures (P/P_0) of 0.4, indicating the presence of mesoporosity. The hysteresis loops of the N_2 adsorption–desorption isotherms of the solids were of type E of the de Boer classification, as shown in Fig. 1A; the pore size distribution, calculated from the BJH method [22], varied slightly upon the different solid modifications and is shown in Fig. 1B. Selected data are shown in Table 1.

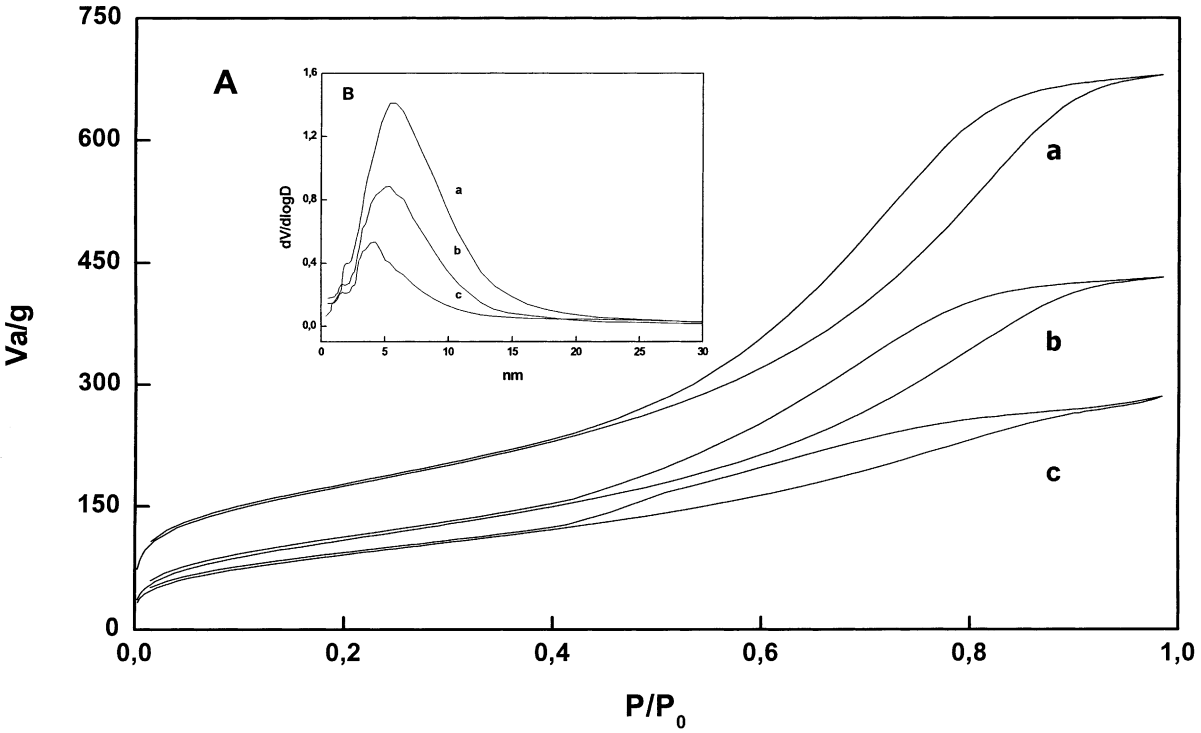

Fig. 1. (A) N_2 adsorption–desorption isotherms of: (a) silica; (b) phosphinated silica; (c) catalyst Rh–P–Si. (B) Pore size distribution curves of: (a) silica; (b) phosphinated silica; (c) catalyst Rh–P–Si.

3.2. FT-IR

The FT-IR spectra obtained for catalyst "Rh–P–Si" are shown in Fig. 2. The spectra show an intense broad peak in the energy region of CO bond vibrations (ν_{CO}). This peak is the result of the contribution of several "Rh–CO" species. After careful deconvolution of the spectra, peaks centred at 2082, 2048, 1997 and 1968 cm^{-1} were obtained. The band at 1968 cm^{-1} was assigned to a [OC–(S)Rh–P–SiO_2] fragment, arising from the reaction of the [Rh(SpymMe$_2$)(CO)$_2$] complex with the phosphinated linker, rendering the expected monocarbonylic monophosphinated complex; this is analogous to the [Rh(SpymMe$_2$)(CO)(PPh_3)] described previously [19], whose CO band appears at 1968 cm^{-1}. Similar complexes have previously been proposed for the tethering process of analogous thiolate Rh complexes on phosphinated modified SiO_2 [16]. The bands centred at 1997 and 2082 cm^{-1} were assigned to the Rh precursor complex adsorbed onto the SiO_2 support that have not reacted with the phosphinated linker. In the spectrum, the energy distance between the CO bands (85 cm^{-1}) is lower than the one in the precursor complex (93 cm^{-1}), possibly due to some ligand constraints in the solid. The band at 2048 cm^{-1} was assigned to a linear CO absorbed on Rh reduced species. In order to study the stability of these species under the reaction conditions, the catalyst was exposed to CO and H_2 pulses at 343 K. Selected spectra are shown in Fig. 2. Spectrum a was obtained in a He atmosphere

Table 1
S_{BET}, porous distribution and pore volume for the described solids

Solid	S_{BET} ($m^2\,g^{-1}$)	Pore size (nm)	V ($cm^3\,g^{-1}$)
SiO_2	627	3–15	1.05
SiO_2–P	488	3–15	0.66
Rh–P–Si	338	3–15	0.44

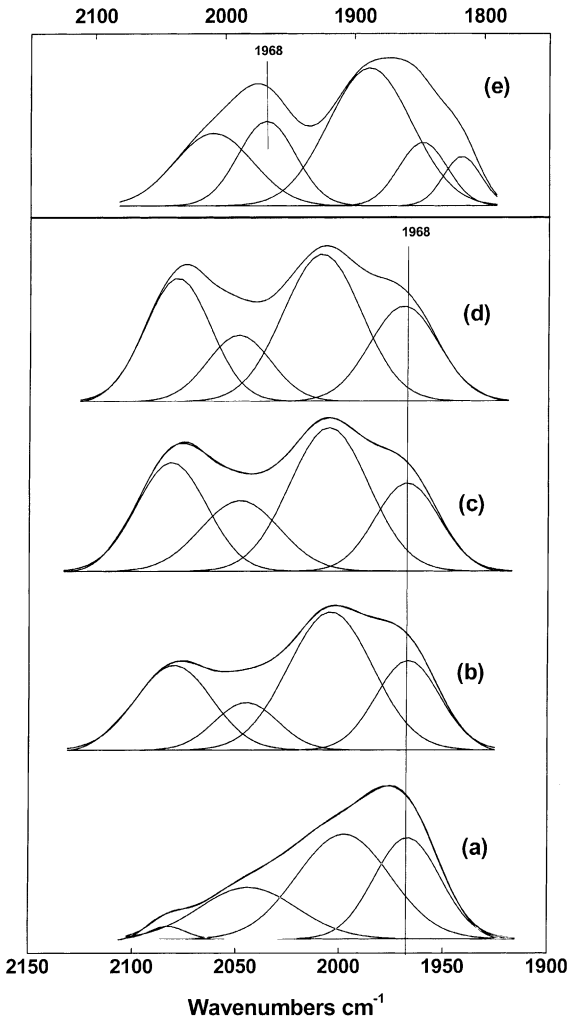

Fig. 2. FT-IR spectra in the carbonyl region of catalyst Rh–P–Si after: (a) fresh sample after outgassing at 343 K and admittance of a pulse of He; (b) CO pulse at 343 K; (c) H_2 pulse at 343 K; (d) $CO + H_2$ pulse at 343 K; (e) spectra of the used catalyst (sample used 4).

at 343 K after gas evacuation. When a pulse of CO was admitted, spectrum b, the intensity of the band at higher wavenumbers was increased while its position remained stable. After gas evacuation, H_2 was admitted at 343 K, and spectrum c was recorded. The intensity of the band at 2048 cm^{-1} increased, thus confirming its initial assignment to a linear CO species adsorbed onto reduced rhodium sites. These species may have been formed after a dissociative reduction of the "–Rh(CO)–" precursor, possibly during the tethering process in the presence of CO [23]. After gas evacuation, the sample was exposed to a mixture of CO and H_2 atmospheres, spectrum d. The spectrum recorded revealed the same species as described above. Spectrum e displayed the carbonyl region of the used catalyst ("used P", catalyst used with addition of PPh_3). After deconvolution of the broadband in the high frequency CO region, several bands were obtained at 2010, 1968 cm^{-1}, and a broad component at lower wavenumbers $\nu_{CO} < 1850\ cm^{-1}$ was ascribed to the Rh_n–CO region. Although unequivocal assignment of these bands was complicated from the band at 1968 cm^{-1}, it seems that the Rh–CO species remaining in the solid were the initial [OC–(S)Rh–P–SiO_2] species, thus confirming the stability of the structure after the catalytic reaction, and also linear Rh–CO species associated with the band at 2009 cm^{-1}. The displacement of this band towards lower wavenumbers is possibly due to the decrease in the dipole–dipole CO coupling [24], since in the used catalyst, the presence of reaction products adsorbed in the catalyst would have reduced CO adsorption [25]. The gem–dicarbonilic species, observed in the spectrum of the fresh solid (spectrum a) and assigned to the presence of [Rh(SpymMe$_2$)$(CO)_2$], had disappeared from the spectrum. This process would have occurred during the early stages of the catalytic cycle, since they are only weakly adsorbed in the solid surface; they would also be responsible for the bridged Rh_n–CO species, whose FT-IR bands were centred at lower frequencies.

3.3. Surface analysis by XPS

The XPS spectra of selected fresh and used catalyst samples were recorded with a view to gain insight into the nature of the chemical species and also their surface concentrations. Selected data are shown in Table 2. The fresh sample displayed its Rh $3d_{5/2}$ core level at a binding energy of 308.9 eV, which can be assigned to a Rh^+ species. The P 2p level showed two components at 132.0 and 132.7 eV, suggesting two phosphine environments. The same occurred for the N 1s peak, which exhibited two components at 398.8 and 399.9 eV. However, S 2p displayed a single component of sulphided species. Precise analysis of the atomic ratios of the former atoms in the sample

Table 2
Binding energy (eV) of core electrons

Solid	Rh $3d_{5/2}$	S 2p	N 1s	P 2p	Si 2p
Rh–P–SiO_2[a]	308.9	162.8	398.8 (39), 399.9 (61)	133.2 (52), 132.0 (48)	103.4
Used[b]	309.4	–	399.1 (47), 400.5 (53)	133.0	103.4
Used P[c]	308.9 (66), 306.8 (34)	161.4	399.0 (56), 400.4 (44)	131.9 (58), 133.3 (42)	103.4

[a] Fresh catalyst.
[b] Catalyst used without the addition of PPh_3.
[c] Used catalyst (during four consecutive reaction cycles) with addition of PPh_3 ($PPh_3/Rh = 4$).

revealed that the N/Rh atomic ratio was 2.2, which is close to the stoichiometric value (N/Rh = 2) from the rhodium precursor. However, the Rh/S atomic ratio in the fresh catalyst was found to be 0.32, a value lower than the theoretical one of 1.0. In addition, the N/S ratio had a value of 7, which was substantially higher than the expected value of 2. The P/S atomic ratio value was 1.3, while the Rh/P atomic ratio value was 2.4. The catalyst used in the hydroformylation of 1-heptene in the presence of PPh_3 ($PPh_3/Rh = 20$) was also analysed (used P). The Rh $3d_{5/2}$ peak exhibited two components at 308.9 (66) eV and 306.8 (34) eV, assigned to Rh^+ and Rh reduced species, respectively. When the catalyst was used without the addition of PPh_3 at 8 bar total pressure (sample "used"), only one Rh peak at 309.4 eV was detected. The intensity of the S 2p peak was very low in the spectra of the "used P" catalyst, and vanished for the "used" catalyst. This feature is indicative of the continuous removal of the S atom from the catalyst surface during the hydroformylation reaction. A similar kind of behaviour has been observed with an analogous catalyst anchored to different supports [13]. The Rh $3d_{5/2}$ core level spectra are depicted in Fig. 3 and the BE of selected samples are shown in Table 2. The surface atomic ratios are summarised in Table 3.

Table 3
XPS surface atomic ratio

Solid	Rh/Si	P/Si	N/Si	S/Si
Rh–P–SiO_2[a]	0.101	0.042	0.223	0.032
Used[b]	0.019	0.046	0.099	–
Used P[c]	0.012	0.026	0.038	0.008

[a] Fresh catalyst.
[b] Catalyst used without the addition of PPh_3.
[c] Used catalyst (during four consecutive reaction cycles) with addition of PPh_3 ($PPh_3/Rh = 4$).

3.4. Catalytic activity

We undertook the study of the catalytic behaviour of the Rh–P–Si system in the hydroformylation of 1-heptene under various reaction conditions similar

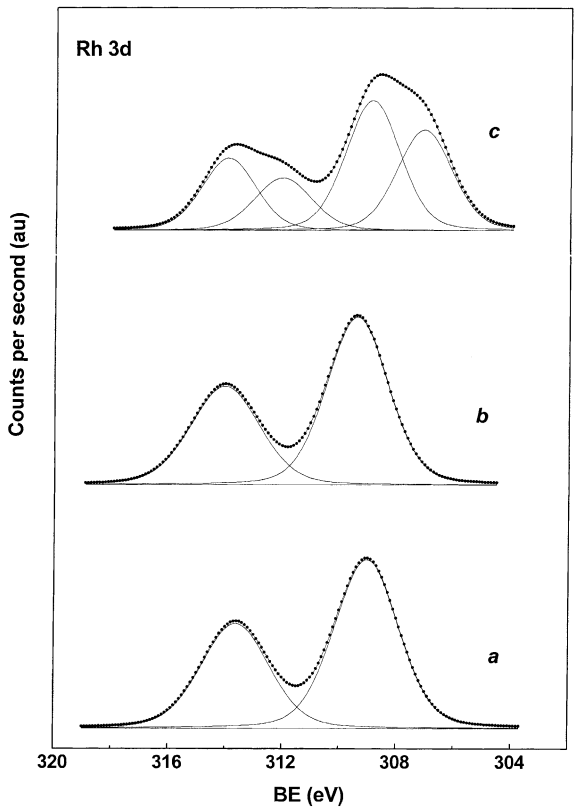

Fig. 3. Rh 3d core-level spectra of selected samples: (a) fresh catalyst Rh–P–Si; (b) "used", corresponding to the catalyst used in the hydroformylation of 1-heptene at 8 bar without the addition of PPh_3; (c) "used P", corresponding to the catalyst used in the hydroformylation of 1-heptene at 30 bar with the addition of PPh_3.

to those previously described for the behaviour of the complex [Rh(SpymMe$_2$)(CO)$_2$] in a homogeneous medium [19]. Under the experimental conditions used, the complex [Rh(SpymMe$_2$)(CO)$_2$] was not active in the hydroformylation reaction unless PPh_3 was added to the reaction medium. However, when Rh–P–Si system was used as a catalyst in the hydroformylation of 1-heptene (30 bar ($H_2/CO = 1$); 343 K) during three reaction cycles, total conversion was achieved for each reaction cycle without the addition of external PPh_3; aldehydes were the main product detected. The product distribution is shown in Table 4 (in Table 4, each reaction is defined by the combination of the reaction and run columns). When the liquid phase collected after each reaction cycle was studied by FT-IR, no bands ascribed to a Rh–CO bond were detected. However they were found to be active in the hydroformylation reaction under similar conditions in the first cycle—reaction I D1—thus confirming a leaching process of the rhodium species during the heterogeneous process. Although the reaction conducted with the liquid phase was faster than the one catalysed by the solid, the final conversion was lower; a value of 89% being achieved. In addition, the product distribution obtained was slightly different to that of the parent cycle.

When PPh_3 ($PPh_3/Rh = 1:20$) (reactions III and IV, 1–5 and 1–4, respectively) was added to the reaction medium, the activity of catalyst Rh–P–Si was followed over five consecutive reaction cycles. Conversions of around 90% were found for each reaction cycle. Fig. 4 shows the 1-heptene conversion profiles obtained with catalyst Rh–P–Si in the third cycle as

Table 4
Some kinetic data for 1-heptene hydroformylation with Rh–P–Si catalyst (the nomenclature of each reaction is a combination of the two first columns)[a]

Reaction	Run[b]	PPh_3[c]	P (bar)	Time (h)	Conversion (%)[d]	Q (%)[e]	n/i[f]	TOF[g]
I	1	0	30	8.3	96	93	2.2	28.6
	2	0	30	17.9	95	94	2.0	13.4
	3	0	30	16.7	97	97	1.9	15.0
	D1	0	30	6.7	89	95	1.8	
II	1	0	8	93.3	77	30	4.5	0.7
	2	1	8	64.0	99	97	3.8	4.3
	3	2	8	42.7	98	99	5.0	6.1
	4	4	8	48.3	98	99	5.1	5.4
	D1	0	30	7.5	86		1.9	
III	1	3	30	8.8	89	93	2.7	2.5
	2	3	30	24.9	81	99	4.7	8.6
	3	3	30	25.7	90	92	3.3	8.5
	4	3	30	48.3	81	99	4.8	4.5
	5	3	30	67.5	89	99	4.6	3.5
	D1	0	30	43.5	99	99	1.8	
	D2	0	30	43.0	78	99	1.9	
IV	1	20	30	20.9	100	100	5.3	12.7
	2	20	30	29.8	79	99	5.3	8.4
	3	20	30	51.3	81	99	5.2	4.2
	4	20	30	79.2	85	100	5.3	2.0
	D1	0	30	25.3	96	100	1.9	

[a] Catalyst Rh–P–Si (1.24×10^{-3} M); 343 K.
[b] Number of the cycle of the reaction; D is for the homogeneous process with the liquids of the corresponding cycle as catalyst.
[c] PPh_3/Rh molar ratio.
[d] 1-Heptene conversion (%).
[e] Chemoselectivity (mol aldehydes/$\sum$ mol products).
[f] n/i (mol linear aldehydes/$\sum$ mol aldehydes).
[g] Maximum turn-over frequency (mol aldehydes/mol Rh × h) in every reaction, no Rh loss were considered within the calculation of the TOF in each cycle.

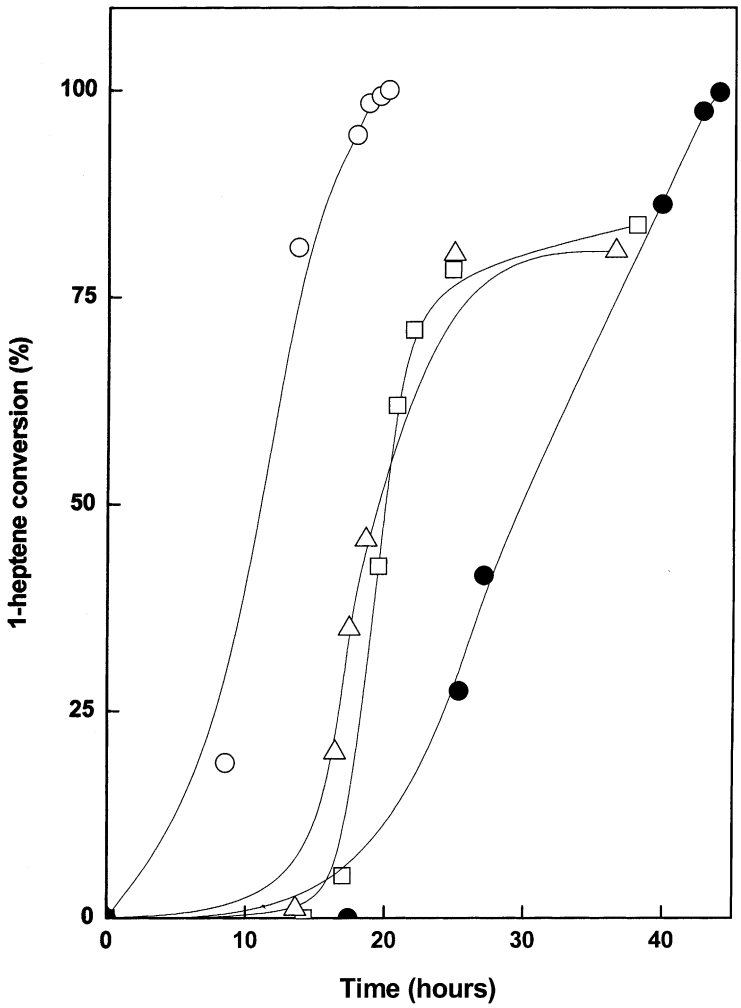

Fig. 4. 1-Heptene conversion profiles monitored during the second cycle of the reaction with catalyst Rh–P–Si at 343 K and (○) $P = 30$ bar, $PPh_3/Rh = 0$; (△) $P = 30$ bar, $PPh_3/Rh = 1$; (□) $P = 30$ bar, $PPh_3/Rh = 20$; (●) $P = 8$ bar, $PPh_3/Rh = 1$.

a function of the amount of PPh_3 and the reaction pressure. Aldehydes were the main products detected. The reaction rate was seen to decrease along the cycles. The addition of PPh_3 increased the *n*/*i* ratio from a value of ca. 2.0 when no PPh_3 was added to the reaction medium (reaction I, 1–3) to ca. 4.5 or 5.3 when 1 or 20 mol PPh_3/Rh was added (reactions III and IV, 1–5 and 1–4, respectively). As expected, the presence of external PPh_3 decreased the reaction rate. The liquids collected after the second cycle—reaction IV D1—were active in the hydroformylation reaction of 1-heptene under similar reaction conditions. Again, lower conversions and *n*/*i* ratios (85% and 1.3, respectively) were obtained as compared to the heterogeneously catalysed cycle. Fig. 5 shows the *n*/*i* ratios obtained in the third cycle of each heterogeneous reaction and that obtained with the homogeneous process after the second reaction cycle.

When the reaction was conducted at lower pressure ($P = 8$ bar) with no addition of PPh_3, (reaction II, 1) only 77% conversion was achieved. Under these conditions, aldehydes were detected, although

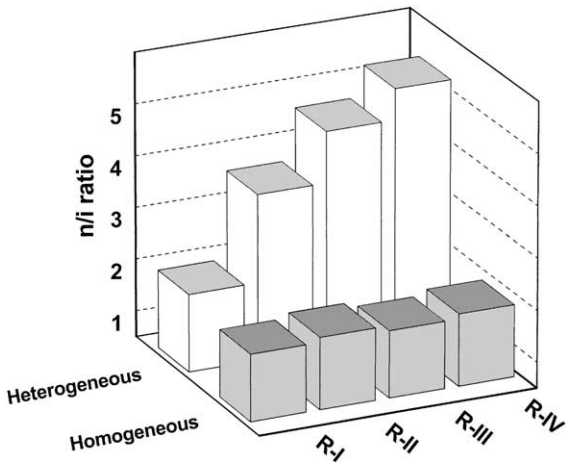

Fig. 5. *n*/*i* ratios obtained after the second cycle of the hydroformylation of 1-heptene catalysed with solid Rh–P–Si (heterogeneous) and the liquid phase collected after the second reaction cycle (homogeneous).

the chemoselectivity (production of aldehydes/total products) was low: ca. 30%. The addition of PPh_3 to the reaction medium increased the chemoselectivity up to a value close to 100%, similar to the values found when the reaction was conducted at 30 bar. The PPh_3/Rh mole ratios were 0, 1, 2 and 4 in each cycle (reaction II, 1–4, respectively). In this case, the addition of PPh_3 markedly increased the TOF (turn-over frequency) of the reaction since aldehyde production was enhanced. An *n*/*i* value close to 4.5 was obtained when $PPh_3/Rh = 1$. Further addition of PPh_3 resulted in a decrease in this value to 3 and 2.9 when $PPh_3/Rh = 2$ or 4 were added, respectively.

4. Discussion

The reaction of the complex $[Rh(SpymMe_2)(CO)_2]$ with the phosphine-modified SiO_2 surface renders the catalytic system Rh–P–Si by substitution of one CO ligand of the former by the PR_n linker of the latter, according to the pathway shown in Scheme 1. However, according to the FT-IR and XPS data during the reaction species, other than this were also formed. From the FT-IR data (spectrum a), it is clear that some of the Rh precursor complex was physically adsorbed onto the solid (bands at 1997 and 2082 cm^{-1}); some "Rh–CO" fragments were also detected. By the XPS data, only Rh^+ species were observed in the catalyst surface; the Rh/N atomic ratio was 2.2, in accordance with the stoichiometry of the pyrimidine complex. However, the Rh/S atomic ratio was slightly higher than expected. This is consistent with a partial displacement of the S atom out of the complex during the anchoring process. Furthermore, in the P region two species were detected. One of them, which was oxidised (132.7 eV), may be indicative of some "–P(S)–" fragments, although from the XPS data "–P(O)–" species could also be proposed. The other one (132.0 eV), ascribed to "–P–Rh–" fragments, resulted from the reaction of the Rh precursor complex with the P atom of the modified support. After the solid Rh–P–Si had been used in the hydroformylation of 1-heptene, the FT-IR spectra revealed that the precursor complex $[Rh(SpymMe_2)(CO)_2]$ detected in the fresh catalyst had been displaced out of the solid: only "Rh–CO", "Rh_n–(CO)" and "OC–(S)Rh–P–SiO_2" species were detected. When a sample of "used P" (used catalyst with PPh_3, reaction IV, 4) was studied by XPS, both reduced and Rh^+ species were detected. However, when the catalyst was used without PPh_3 ("used" sample, reaction II, 1), only one Rh species at 309.4 eV was detected. Since in the former case, hydroformylation proceeded successfully, while in the latter the major product detected after the reaction were heptene isomers, it seems likely that the reduced "Rh–CO" species must play an important role in hydroformylation. This was explained by Chuang and Pien [25], studying the hydroformylation of ethylene by a Rh-supported catalyst, by the facility of linear CO species to participate in the CO insertion step.

By XPS, almost no S was detected either in the "used P sample" or in "used" sample. This apparent contradiction between the assignment of the FT-IR band of the used catalyst at 1968 cm^{-1} as a "OC–(S)Rh–P–SiO_2" fragment and the absence of S in the XPS analysis may be explained by considering that the XPS technique affords information about the outer surface of the solids. This could mean that during/after the catalytic reaction, the surface catalytic species were not in the "–Rh–S–" form, i.e., the rhodium thiolate was not the active catalyst. However, "OC–(S)Rh–P–SiO_2" was clearly detected both in the fresh and used samples, although it is consumed during the reaction. Since such species is not proposed

as the active catalytic species, the role of such Rh thiolate fragments in the solid could be pictured as a pool of Rh in the catalyst.

Unfortunately, when the leaching of the rhodium was analysed by ICP techniques, unclear results were obtained. Rh contents of 0.5 and 3.8 wt.% were obtained after two consecutive hydroformylation cycles. The presence of some high boiling temperature compounds that are presumed to be formed along the catalytic cycles caused an incomplete solid segregation, thus obtaining inexact analytical results.

Since the liquid phase collected after the reaction with the Rh–P–Si catalyst was active in 1-heptene hydroformylation, it was evident that some Rh had occurred. This leaching process was attributed in the first reaction cycles to the Rh precursor complex adsorbed onto the solid, and was confirmed by the FT-IR spectra of the fresh and used catalyst. In these reactions, i.e., homogeneous process, the product distribution was different to that obtained when the reaction was conducted in the presence of the Rh–P–SiO_2 catalysts, i.e., heterogeneous process. This was indicative of the different nature of the catalytic species present in both media. As expected, the homogeneous process was faster, since in the liquid phase, the catalyst is already activated right from the beginning. The low *n*/*i* ratio value of the liquid-phase hydroformylation process could not be ascribed to the non-addition of PPh_3, since most of it was present in the liquid phase collected after the heterogeneous reaction. It seems reasonable to expect that at some point during the heterogeneous process, some homogeneous reaction was also taking place and even though the homogeneous process was faster than the heterogeneous one, the product distribution after the reaction did not become regulated by the one of the homogeneous process but, instead, by the heterogeneous one. This feature may suggest a low contribution of the homogeneous reaction, i.e., a low Rh leaching during the hydroformylation process.

According to the XPS data (Table 3), the Rh content of the fresh sample was diminished by ca. four times after the reaction (four cycles), whereas according to the FT-IR data, the band centred at 1968 cm^{-1}, which is ascribed to "OC–(S)Rh–P–Si", decreased by only ca. 1.5-fold. Although difficult to quantify, the Rh leaching process was taking place along the reaction, especially during the first reaction cycle, in which some physically adsorbed complex on the solid surface would have become easily solved. However, the heterogenisation of the Rh complex results in an active catalyst precursor whose activity in the hydroformylation of 1-heptene was maintained at least for five consecutive reaction cycles.

5. Conclusions

The [$Rh(SpymMe_2)(CO)_2$] complex was tethered to a phosphine-modified SiO_2 support, yielding a Rh–P–Si catalyst precursor that proved to be active in the hydroformylation of 1-heptene. During the anchoring process, different Rh species were formed. In some of them, the S atom was removed from the complex. It was observed that Rh leaching occurs, especially during the first reaction cycle, when the adsorbed [$Rh(SpymMe_2)(CO)_2$] complex was still present on the catalyst surface. The addition of PPh_3 renders the reaction more selective towards the production of aldehydes, favouring the stabilisation of linear "Rh–CO" species. The formation of a "OC(S)–Rh–P–SiO_2"-like structure upon reaction of the Rh precursor and the SiO_2 linker acts as a pool of Rh during the catalytic process. It seems that the removal of the S atom from the complex may render the active catalyst on the outer surface of the support. Although the Rh–P–Si solid may not be the active catalytic species, it can be proposed as an effective heterogeneous hydroformylation catalyst precursor.

Acknowledgements

We gratefully acknowledge financial support from CICYT project QUI98-0877.

References

[1] P. Kalck (Guest Ed.), Recent Achievements in Carbonylation Reaction, J. Mol. Catal. A 143 (1999).
[2] B. Cornils, W.A. Herrmann, in: B. Cornils, W.A. Herrmann (Eds.), Applied Homogeneous Catalysis with Organometallic Compounds, Vol. 1, Wiley/VCH, New York, 1996, p. 575 (Chapter 3.1.1).
[3] B.E. Hanson, J.R. Zoeller (Eds.), Phase Separable Homogeneous Catalysis, Catal. Today 42–44 (1998).

[4] I.T. Horváth (Ed.), Catalysis in Water, J. Mol. Catal. A 116 (1997).
[5] B. Cornils, W.A. Herrmann (Eds.), Aqueous-Phase Organometallic Catalysis, Concepts and Applications, Wiley/VCH, New York, 1998.
[6] B. Cornils, E. Wiebus, CHEMTECH, January (1995) 33.
[7] P. Purwanto, H. Delmas, Catal. Today 24 (1995) 135.
[8] O. Wachsen, K. Himmler, B. Cornils, Catal. Today 42 (1998) 373.
[9] T.M. Hertz, Topics Catal. 4 (1997) 187.
[10] N. Yoneda, Y. Nakagawa, T. Mimami, Catal. Today 36 (1997) 357.
[11] M.E. Davis, P.M. Butler, J.A. Rossin, B.E. Hanson, J. Mol. Catal. 31 (1985) 385.
[12] J.A. Díaz, M.C. Román-Martínez, C. Salinas-Martínez de Leca, J. Mol. Catal. A 171 (2001) 81.
[13] S. Rojas, S. Murcia-Mascarós, P. Terreros, J.L.G. Fierro, New. J. Chem. 25 (2001) 1430.
[14] S. Bischoff, A. Köckritz, M. Kant, Topics Catal. 13 (2000) 327.
[15] J. Balué, J.C. Bayón, J. Mol. Catal. A 137 (1999) 193.
[16] H. Gao, R. Angelici, J. Mol. Catal. A 149 (1999) 63.
[17] H. Gao, R. Angelici, Organometallics 17 (1998) 3063.
[18] J.L.G. Fierro, M.D. Merchán, S. Rojas, P. Terreros, J. Mol. Catal. A 166 (2001) 255.
[19] S. Rojas, R. Fandos, A. Rodriguez, P. Terreros, J.L.G. Fierro, J. Chem. Soc., Dalton Trans. 15 (2000) 2316.
[20] M. Čapka, Syn. React. Inorg. Metal-Org. Chem. 7 (4) (1977) 347.
[21] B. Marciniec, Z. Foltynowicz, W. Urbaniak, J. Perkowski, Appl. Organomet. Chem. 1 (1987) 267.
[22] S.G. Gregg, K.S.W. Sing, Adsorption, Surface Area and Porosity, Academic Press, New York, 1982.
[23] S. Trautmann, M. Baerns, J. Catal. 150 (1994) 335.
[24] F. Stoop, F.J.C.M. Toolenaar, V. Ponec, J. Catal. 73 (1982) 50.
[25] S.S.C. Chuang, S.I. Pien, J. Catal. 135 (1992) 618.